Dynamics of Deep-Bed Filtration

Part I: Analysis of Two Limiting Situations

HSU-WEN CHIANG and CHI TIEN

Department of Chemical Engineering and Materials Science Syracuse University Syracuse, NY 13210

The dynamic behavior of deep-bed filtration was studied by considering two limiting situations. In the first case it was assumed that deposition leads to the presence of a reasonably smooth deposit layer over filter grains. In the second case particle aggregates, once formed, were assumed to remain rigid and the deposited particles to act as additional collectors. The effect on filter performance of the media change resulting from the presence of these two types of deposits was examined quantitatively.

SCOPE

One of the ultimate objectives of the study of deep-bed filtration is to achieve a predictive capability of the dynamic behavior of the process. As the retention of particulates within a filter bed increases, the structure of the filter media undergoes a continuous change, including both the shape and size of the pore species as well as possibly the physiocochemical conditions at the filter grain surfaces. These changes, in turn, affect the flow of suspension through the media, the transport of particles from the suspension to the filter grain surface, and their subsequent deposition, giving rise to the time-dependent behavior of the filtrate quality and the pressure drop across the bed for a constant flow throughput.

In this study, the effect of particle deposition on the dynamic behavior of deep bed filters was examined by considering two limiting situations. In the first instance, particle deposits outside filter grains were assumed to form relatively smooth coatings. The physical process can be described as a moving-boundary problem, the solution of which yields information concerning the continuous changes of the collector shape and size and the flow field around the collector as well as the rate of particle retention and pressure drop.

In the second limiting situation, details of the deposition process were described by a stochastic model proposed earlier (Tien et al., 1977; Wang et al., 1977; Pendse and Tien, 1982). The concept of adhesion probability (Gimbel and Sontheimer, 1978) was incorporated to account for the possibility that contact between particles and filter grains may not necessarily lead to deposition. The structure of the deposits, once formed, was assumed to be rigid. In both cases, interception was considered to be the dominant collection mechanism.

The results obtained from both situations were presented in the form of increases in collection efficiency and pressure gradient as functions of the extent of deposition described by the specific deposit. The results can be readily used to predict the dynamic behavior of deep bed filters.

CONCLUSIONS AND SIGNIFICANCE

The analysis presented in the paper yields information relating the changes of the unit collector efficiency and pressure gradient of deep bed filters as functions of the extent of particle retention. Accordingly, the information can be applied to predict the histories of filtrate quality and pressure drop across filter beds for a given set of operating and system variables.

The results of this study also demonstrated the significant effect of deposit morphology on the filter performance. Tested against experimental data, as shown in Part II, the results of the two limiting situations were found to bracket the experimental data, thus suggesting the possibility that a combination of these results may offer a viable way of predicting the dynamic behavior of deep bed filters.

Hsu-Wen Chiang is currently with Whiteshell Nuclear Research Establishment, Atomic Energy of Canada Ltd., Pinawa, Manitoba, ROE 1L0, Canada.

INTRODUCTION

A major unresolved problem in deep-bed filtration is the effect of particle deposition on filter performance and, specifically, the development of a capability for predicting the histories of the effluent quality and pressure drop across the filter bed. Experimentally, these quantities have shown to exhibit strong time-dependent behavior as a filter bed becomes increasingly clogged.

A number of investigators have examined the effect of particle deposition experimentally. Empirical expressions which account for the effect of deposition on the filter coefficient and the presence gradient (see Table 1 of Pendse, 1979) have been proposed. These equations in general have only limited utility since they are based on data obtained under rather specific conditions. More recently, a phenomenological model of deep bed filtration was proposed by Tien et al. (1979). The phenomenological model was found capable of describing both the enhancement and deterioration of filtration quality over time as observed in experiments. It also agreed well with experimental data. The agreement, however, was achieved through the use of two adjustable parameters. Since these parameters cannot be predicted a priori, the phenomenological model cannot be used as a truly predictive tool necessary for design calculations.

The accumulation of deposited particles within a filter bed causes changes in the structure of the filter media. The qualitative effect of these changes on filter performance can be summarized as follows:

1. The presence of deposited particles modifies the geometry and surface conditions of the filter grains. Both of these changes affect the collection of particles.
2. The change of the filter grain geometry imparts a change in the flow fields around the filter grains. Both the drag force to which the filter grains are subjected and the collection efficiencies of the filter grains depend upon the flow field.
3. Deposited particles may act as additional collectors. Their presence therefore enhances filter performances. At the same time, the drag forces to which they are subjected imply a corresponding pressure drop increase.
4. As the size of the particle deposits increases, the drag force acting on the deposits increases correspondingly. Some of the deposited particles may be reentrained. Equally likely certain parts of the deposit may be bent, thus altering the structure of the aggregate formed by the deposited particles.

A rigorous analysis of the effect of particle deposition on filter performance therefore should include all the features mentioned above. While this approach can in principle be implemented by solving the appropriate equations of fluid and particle motion, neither the mathematical techniques necessary for the solutions of these equations nor the knowledge of the nature of the interaction forces between filter grains and particles and between particles themselves is available. Practically speaking, the problem can be analyzed only under simplified and idealized conditions.

The present work studied the effect of particle deposition on filter performance by examining two limiting situations. In the first case, particle collection on filter grains results in the formation of a reasonably smooth deposit layer outside the filter grains. This approach represents a generalization of the earlier work of Tien et al. (1979), which assumed particle deposition in the form of uniform coating over filter grains, and is similar to the work of Payatakes et al. (1977). The latter work yielded only limited results because of computational difficulties. The present work provides a new formulation which overcomes the earlier difficulties. Furthermore, the effect of collector geometry was considered as part of the study.

For the second limiting situation, it was assumed that the build-up of particle deposits can be described by the hypothesis advanced by Tien et al. (1977) and Wang et al. (1977) and subsequently applied in the study of aerosol filtration (Pendse and Tien, 1982; Tsiang et al., 1982). The adhesion probability concept (Gimbel and Sontheimer, 1979) was incorporated into this analysis in order to determine the result once a particle is transported and impacts on a filter grain. The particle deposit, once formed, remains rigid and intact.

In carrying out analysis of both limiting situations, the researchers used the constricted tube model of Payatakes et al. (1973) to characterize the filter media. The results of the analyses are presented in forms suitable for predicitng the dynamic behavior of deep-bed filtration.

What follows is a brief outline of the phenomenological equations describing the dynamic behavior of deep-bed filtration, followed by the results of analyses of the two limiting situations.

PHENOMENOLOGICAL EQUATIONS OF DEEP-BED FILTRATION

The phenomenological equations describing the dynamic behavior of deep-bed filtration of a suspension of monodispersed particles in a filter bed initially free of deposited particles are, according to Tien and Payatakes (1979):

$$u_s \frac{\partial c}{\partial z} + \frac{\partial \sigma}{\partial \theta} = 0 \tag{1}$$

$$\frac{\partial \sigma}{\partial \theta} = -u_s \lambda c \tag{2}$$

$$\Delta p = \int_0^L \left(\frac{\partial p}{\partial z}\right) dz \tag{3}$$

$$c = c_{in}, \quad z = 9; \quad \sigma = 0, \quad z \geq 0, \quad \theta \leq 0 \tag{4}$$

$$\theta = t - \int_0^z \frac{dz}{u/\epsilon} \tag{5}$$

where c and σ denote the particle concentration of the suspension and the specific deposit, i.e., amount of particle deposited per unit volume of filter bed. λ is the so-called filter coefficient and is known to be a function of the extent of deposition. The meanings of other symbols are given in the Notation section.

The twin features of the dynamic behavior of deep-bed filtration are the histories of the effluent quality and the pressure drop necessary to maintain a constant flow rate. In principle, this information can be obtained from the solution of Eqs. 1–5, which in turn requires efficient numerical algorithms as well as numerical values of λ and $(\partial p/\partial z)$. Numerous studies have been made to develop such algorithms (Lapidus, 1962; Lister, 1962; Vanier, 1970; Herzig et al., 1970). Thus, satisfying the second requirement represents the main thrust of current deep-bed filtration research.

As stated earlier, the presence of deposited particles affects both the values of λ and $(\partial p/\partial z)$. To account for this effect of particle deposition, one may write

$$\lambda = \lambda_o F_1(\alpha,\sigma) \tag{6}$$

$$(\partial p/\partial z) = (\partial p/\partial z)_o F_2(\beta,\sigma) \tag{7}$$

where the subscript o denotes the initial or clean filter state. The pressure gradient required to maintain a given flow rate through a clean filter bed can be estimated from the Carman-Kozeny equation. Similarly, recent studies (Yao et al., 1971; Spielman and Fitzpatrick, 1973; Payatakes et al., 1974; Rajagopalan and Tien, 1976, 1977) have largely solved the problem of estimating λ_o. On the other hand, determining the functions F_1 and F_2 is, in essence, the quantitative study of the effect of particle deposition on filter performance.

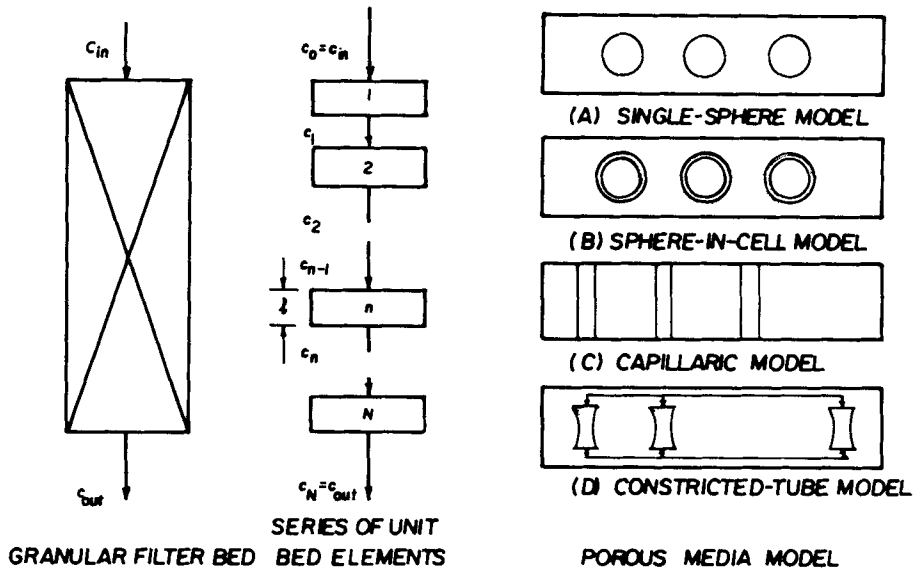

Figure 1. Schematic representation of a granular filter bed with several porous media models.

MODEL REPRESENTATION OF FILTER BED

For carrying out a rational analysis of particle collection in a granular bed, one may describe the bed by the conceptual framework suggested earlier (Tien and Payatakes, 1979). As shown in Figure 1, a filter bed may be considered to be a series of unit bed elements (UBE) which are statistically similar in their initial state. Each element consists of a number of collectors; in the simplest case, these collectors may be assumed to be of equal shape and size. The capability of a filter bed to remove suspended particles from suspensions therefore can be described by the collection efficiencies, η, of these collectors, defined as

$$\eta = \frac{c_{i-1} - c_i}{c_{i-1}} \tag{8}$$

where c_{i-1} and c_i are the particle concentrations entering the ith and $(i+1)$th unit bed elements. The relationship between η and λ is found to be

$$\lambda = \frac{1}{\ell} \ln \frac{1}{1-\eta} \simeq \frac{\eta}{\ell} \quad \text{if } \eta \ll 1 \tag{9}$$

where ℓ is the axial distance corresponding to one unit bed element and is given as (Payatakes et al., 1973).

$$\ell = \left[\frac{\pi}{6(1-\epsilon)} d_g^3\right]^{1/3} \tag{10}$$

Limiting Situation (A)

Basis of Calculation. In limiting situation (A), it is assumed that particle deposition results in the presence of relatively smooth and contiguous deposit layers. In terms of the constricted tube model, this means that the diameter of the tube decreases with time, but the extent of decrease is a local function and varies with time. Let Δ be the thickness of the deposit layer. The change in the deposit thickness can be related to the particle deposition flux, J_i, by the following expression:

$$\frac{d}{dt}[(1-\epsilon_d)(\delta A)(\Delta)] = (\delta A) J_i \hat{v} \tag{11}$$

where δA is an arbitrary surface element on the surface of the constricted tube (see Figure 2), J_i is the particle flux (expressed in number of particles), ϵ_d is the porosity of the deposit, and $\hat{v}$ is the volume of a single deposited particle.

The rate of particle deposition over the area element δA, i.e., $J_i \delta A$, can be found by knowing the trajectories of particles in the suspension as they move through the constricted tube. Referring to Figure 2a, if one assumes that the effect of Brownian diffusion is negligible (namely, the particles to be removed have diameters greater than 1 μm), then one can determine the trajectories of the particles from the integration of the appropriate equations of particle motion. Let curves 1 and 2 denote the trajectories which reach the wall of the tube at $z = z$ and $z = z + \Delta z$, respectfully. Let a and b denote the respective radial positions at the inlet of the constricted tube, from which trajectories labeled 1 and 2 originate. All the particles entering the tube with their radial positions between positions a and b will be deposited over the surface element δA. Now $J_i \delta A$ can be readily determined.

The above-stated principle of calculation can be greatly simplified for deep-bed filtration of liquid suspension of particles of a diameter greater than 1 μm. In such cases, particle collection caused by Brownian diffusion is insignificant; the dominant particle collection mechanism is interception. In other words, particle trajectories coincide with fluid stream lines. The amount of suspension bound by the two trajectories is $2\pi[\psi|_{x+\Delta x, y=d_p/2} - \psi|_{x,y=d_p/2}]$ and the number of particles deposited over δA is

$$I_i = J_i \delta A = 2\pi[\psi|_{x+\Delta x, y=d_p/2} - \psi|_{x,y=d_p/2}] \tag{12}$$

Substituting Eq. 12 into Eq. 11, after some rearrangement one obtains the following expression of the growth of the deposit layer:

$$\frac{d\Delta^*}{dt^*} = \left(\frac{d\psi^*}{dx^*}\right)\Big|_{y^*=N_R/2} \frac{1}{P_w^*} \frac{\hat{v}}{1-\epsilon_d} \tag{13a}$$

$$\delta\Delta^* \simeq \left[\left(\frac{d\psi^*}{dt^*}\right)_{y^*=N_R/2} \frac{1}{P_w^*} \frac{\hat{v}}{1-\epsilon_d}\right] \cdot \Delta t^* \tag{13b}$$

with the meanings of the dimensionless variables given in the Notation. The stream function for flow through a constricted tube with the wall diameter P_w as an arbitrary function of the axial

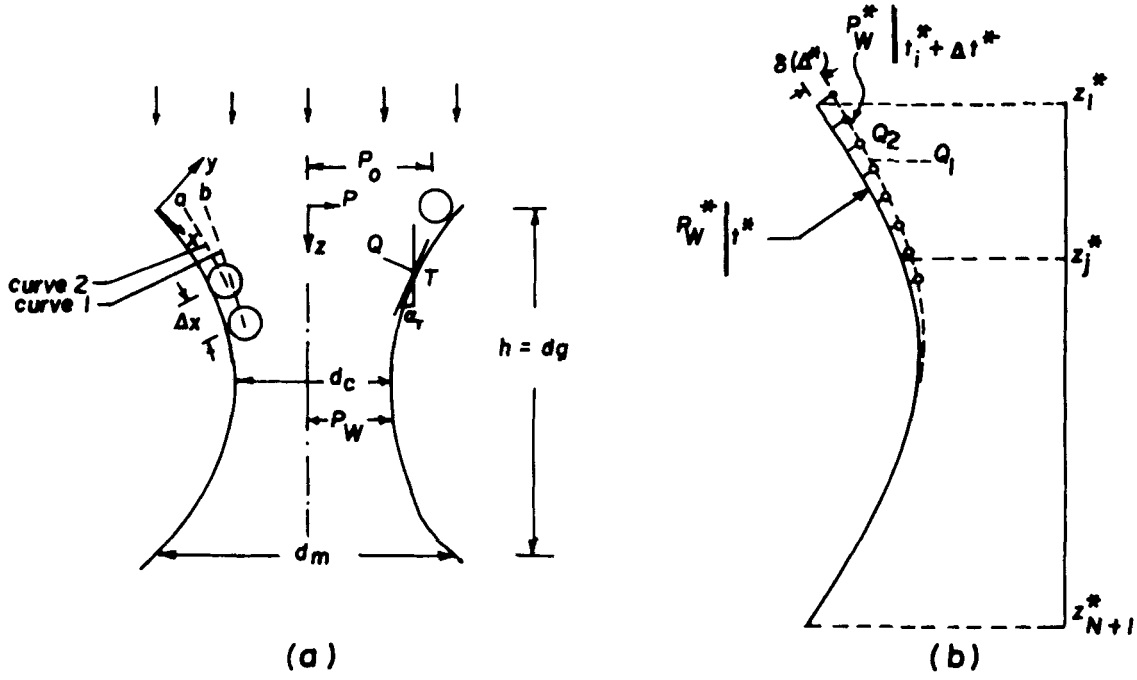

Figure 2. a) Coordinate system for a constricted tube. b) Schemaic diagram of a constricted tube for numerical calculation.

distance was obtained by Chow and Soda (1972). The results can be expressed as

$$\psi' = \frac{\psi}{u_m \cdot p_m^2} = \sum_{n=o}^{\infty} (P_m^*)^n \psi_n'(P', z', N_{Re_m}) \tag{14}$$

The zeroth, first- and second-order solutions are given, respectvely, as

$$\psi_o' = 0.5(R^4 - 2R^2) \tag{15a}$$

$$\psi_1' = (0.25)N_{Re_m}(dP_w'/dz')/P_w' \cdot \left[\left(\frac{1}{9}\right)(R^8 - 6R^6 + 9R^4 - 4R^2)\right] \tag{15b}$$

$$\psi_2' = -0.5[5(dP_w'/dz')^2 - P_w'(d^2P_w'/dz'^2)](R^2 - 1)^2R^2/3 - (0.125)N_{Re_m}[(dP_w/dz')^2/P_w'^2][32R^{12} - 305R^{10} + 750R^8 - 713R^6 + 236R^4]/(3{,}600) \tag{15c}$$

where

$$z' = z/h \tag{16a}$$

$$P' = P/P_m \tag{16b}$$

$$P_w' = P_w/P_m \tag{16c}$$

$$R = P'/P_w' \tag{16d}$$

$$P_m^* = P_m/h \tag{16e}$$

$$N_{Re_m} = u_m P_m \rho/\mu \tag{16f}$$

and h is the height of the constricted tube. In applying the constricted-tube model for media representation, h is the same as d_g.

As shown in Eq. 16f, the Reynolds number is defined in terms of the average velocity through the tube, namely, the volumetric flow rate divided by the average cross-sectional area, πP_m^2. The average tube radius, P_m, is given as

$$P_m = \left[\int_o^h P_w \cdot dz\right]\Big/ h \tag{16g}$$

The relationship between u_m and the superficial velocity through the filter bed, u_s, is

$$u_s = (u_m)(\pi P_m^2) \cdot N_c \tag{17}$$

where N_c is the number of the constricted tubes per unit cross section of the bed. According to Payatakes et al. (1974), N_c is given as

$$N_c = \frac{6\epsilon^{1/3}(1 - S_{w_t})^{1/3} \cdot (1 - \epsilon)^{2/3}}{\pi d_g^2} \tag{18}$$

and S_{w_t} is the so-called fraction of irreducible saturation, obtained from the capillary pressure-saturation data of the filter media.

Similarly the pressure drop across a constricted tube, according to the Chow and Soda solution, is

$$\Delta p' = (\Delta p)P_m/(\rho u_m^2 h) = \sum_{n=o}^{\infty} P_m^{*n}(\Delta p_n') \tag{19}$$

The zeroth, first- and second-order solutions are

$$\Delta p_o' = -(8/N_{Re,m}) \int_o^1 [1/(P_w')^4] \cdot dz' \tag{20a}$$

$$\Delta p_1' = \int_o^1 [4(dP_w'/dz')/(P_w')^5] \cdot dz' \tag{20b}$$

$$\Delta p_2' = (0.5/N_{Re,m})\left[(88 - 96R^2)(1/3)\left\{\frac{1}{P_w'^3}\frac{dP_w'}{dz'}\Big|_{z'=0}^{z'}\right\}\right.$$

$$-\frac{64}{3}\int_o^{z'}\frac{1}{(P'_w)^3}\frac{d^2P'_w}{dz'^2}dz'\Bigg]$$
$$+\ 0.125N_{Re,m}\left[\left\{-\frac{1}{5(P'_w)^5}\frac{dP'_w}{dz'}\Bigg|_{z'=0}^{z'=1}\right\}\frac{8}{9}G(R)\right.$$
$$\left.+\ g(R)\int_o^{z'}\frac{8}{9P'^5_w}\frac{d^2P'_w}{dz'^2}dz'\right] \quad (20c)$$

and

$$G(R) = [23R^8 - 165R^6 + 232.5R^4 - 127.39R^2 + 21.18 \quad (21a)$$

$$g(R) = 0.6R^8 - 9R^6 + 10.5R^4 - 3.478R^2 + 0.236 \quad (21b)$$

As shown in the phenomenological equations given earlier, predicting the dynamic behavior of deep-bed filtration requires knowledge of the functions F_1 and F_2, which account for the effect of particle deposition in collection and pressure drop, respectively. By definition, F_1 and F_2 are

$$F_1 = \frac{\lambda}{\lambda_o} \simeq \frac{\eta}{\eta_o} \quad (22a)$$

$$F_2 = \frac{(\partial p/\partial z)}{(\partial p/\partial z)_o} \simeq \frac{(\Delta p/h)}{(\Delta p/h)_o} \quad (22b)$$

The collection efficiency of the unit collectors can be found from the following expression:

$$\eta = \frac{\psi^*|_{\text{limiting}} - \psi^*|_{z^*=0,P^*=P_o^*}}{\psi^*|_{z^*=0,P^*=0} - \psi^*|_{z^*=0,P^*=P_o^*}} \quad (23)$$

Where $z^* = z/d_g$ and $P_o^*(=P_o/d_g)$ is the further most radial position which can be occupied by a particle at the inlet of the constricted tube. $\psi^*|_{\text{limiting}}$ is the stream function value along the limiting trajectory ("limiting trajectory" having been explained above). Thus, the collection efficiency corresponding to any degree of particle deposition can be calculated from Eqs. 23 and 14, once the tube wall geometry (namely, P_w vs. z) is known. The ratio of η to η_o gives the value of F_1. Similarly, Eq. 19 can be used to calculate the pressure drop across a tube of length of h, and the ratio of the pressure to its initial value gives the value of F_2.

Both functions F_1 and F_2 depend upon the system considered and the operating variables as well as on the extent of particle deposition. Thus, in simulating the dynamic behavior under a particular set of conditions, F_1 and F_2 can be considered as functions of the specific deposit of the bed. The latter quantity, denoted as σ, with the unit of volume of deposited particles per unit volume of bed, can be found from the following expression:

$$\sigma = \left[\frac{V|_{t^*} - V|_o}{\ell/N_c}\right]\cdot(1-\epsilon_d) \quad (24)$$

where

$$V|_o = \int_o^h \pi(P_w)^2_{t^*=0}\cdot dz \quad (25a)$$

$$V|_{t^*} = \int_o^h \pi(P_w)^2\cdot dz \quad (25b)$$

Note that $V|_o$ and $V|_{t^*}$ represent the volume of the constricted tube initially and with any degree of deposition.

Procedure for Calculation. The numerical procedure used for calculating the change of tube geometry with deposition and the subsequent evaluation of F_1 and F_2 as functions of σ can be briefly described as follows: A constricted tube of a particular shape was first chosen. The axial length of the tube was divided into N equal increments with the grid points denoted as $z_1^* = 0, z_2^*, \ldots z_j^* \ldots z_{N+1}^* = 1$. Assume that the wall radius corresponding to z_j^* is $P_w^*(z_j)$ and

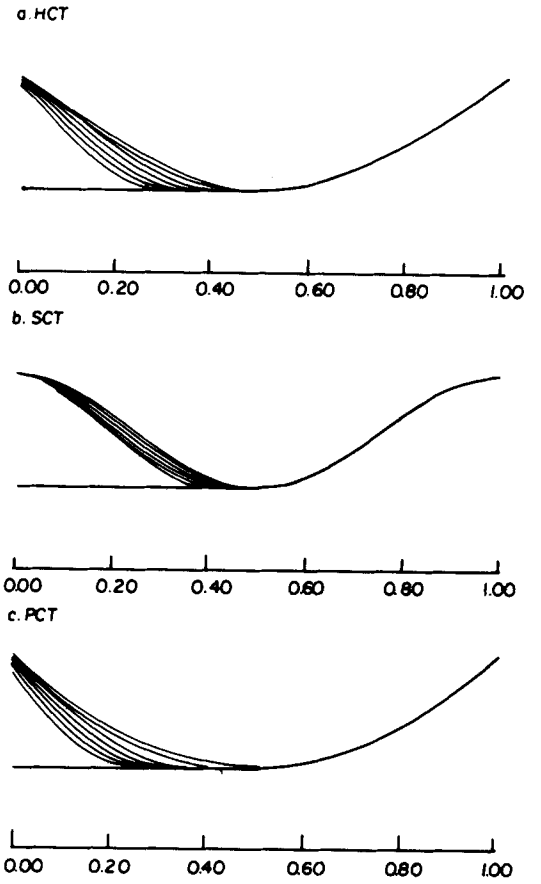

Figure 3. Change in wall profile of a constricted tube resulting from deposition.

that $P_w^*(z_j)$ is known at a given time. The increase in tube thickness $\delta(\Delta^*)$ corresponding to the grid point z_j over a time interval Δt^* was found from Eq. 13b, with the stream function value calculated from Eq. 14 on the basis of the wall profile data at time t^*. This procedure yields a new contour for the tube wall at $t^* + \Delta t^*$, as shown by the points denoted by open circles in Figure 2b. An interpolation method based on the cubic spline scheme was used to obtain the new values of P_w^* (namely, those at $t^* + \Delta t^*$) corresponding to each of the grid points, $z_1^* \ldots z_{N+1}^*$. This procedure can be repeated to obtain the tube wall profile at the end of the next time increment. Furthermore, from the wall profile information at a given time (i.e., P_w^* vs. z^*), the collection efficiency of the tube was calculated from Eq. 23, with the stream function values obtained from Eqs. 14 and 15a–c, and the pressure drop from Eqs. 19 and 20a–c, with R taken to be unity. The wall profile data also permitted the calculation of the specific deposit, σ, from Eqs. 24, 25a, and 25b, establishing the functional relationship between F_1 (and F_2) with σ. Details of the calculation procedures can be found in Chiang (1983).

Results

A number of calculations were made covering a variety of situations. The variables examined include the particle and filter grain diameters, the bed porosity (which determines the dimensions of the constricted tubes) as well as the tube geometries. Three types of constricted-tube (CT) wall geometries were considered in the calculation; namely, parabolic (PCT), hyperbolic (HCT), and sinusoidal (SCT). The results obtained are summarized below.

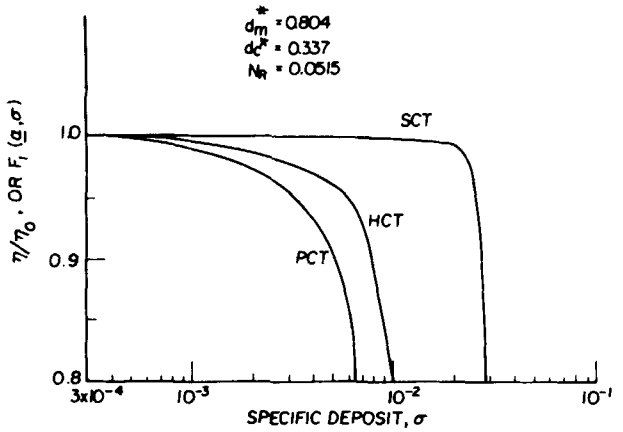

Figure 4. Effect of tube geometry on relationship between F_1 and σ-limiting case (A).

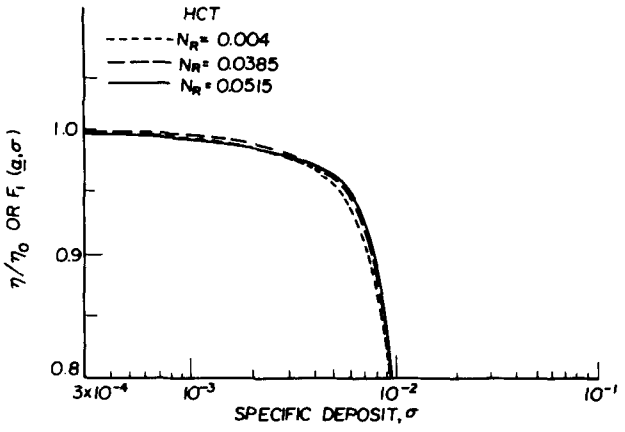

Figure 6. Effect of particle size on relationship between F_1 and σ-limiting case (A).

Change in Tube Geometry Resulting from Particle Deposition. Figures 3a, b, c show the change in the wall profiles resulting from deposition for the three types of constricted tube (HCT, PCT, and SCT). In all three cases, deposition of particles takes place only in the upper half of the tube, since $(d\psi^*/dx^*)_{y^*=N_R/2} \leq 0$ for $0.5 \leq z^* \leq 1$ and all t^*. Therefore, according to Eq. 13b there can be no deposition for $0.5 \leq z^* \leq 1$. Furthermore, for the first half of the tube, the wall radius, P_w^*, was found to decrease with the increase of deposition until the values of P_w^* reached the constriction radius, $d_c^*/2$. Eventually, the upper half of the constricted tube became a cylindrical tube of the diameter d_c^* and the tube became nonretentive. These figures also demonstrated the difference in the growth of the deposits within an SCT and that in an HCT or a PCT. For a sinusoidal contricted tube, the wall radius at $z^* = 0$ hardly changed with time until the whole upper half of the constricted tube became nearly a cylindrical tube. In contrast, for both the HCT and the PCT, the changes in the wall radius near the inlet were more gradual.

Effect of Tube Geometry. The variation in the filter coefficient as a result of deposition, as expressed by λ/λ_o (or F_1) vs. σ for the three different types of constricted tubes, is given in Figure 4. For $\sigma < 3 \times 10^{-3}$, F_1 remained essentially constant for the SCT geometry, while for both the HCT and PCT F_1 decreased gradually with σ. For the HCT and PCT, when σ exceeded 6×10^{-3}, F_1 decreased rapidly with the increase in σ; for the SCT, F_1 changed precipitously when σ reached 0.03. This behavior is a direct consequence of Eq. 23. The collection efficiency depends on the stream function values determined at the center of the particle when the particle is placed on the tube wall at the entrance to the tube and at the constriction. As Figures 3a, b, c illustrate, as σ increased, wall radii at these two points hardly changed at all for an SCT, and the wall radii at the entrances changed gradually for an HCT and a PCT. Thus, F_1 changed only slightly with σ for the SCT and changed gradually with σ for the HCT and the PCT. Furthermore, these figures also show; as the upper half of the constricted tube eventually became a straight tube, the collector became nonretentive. Qualitatively, the results agree with some experimental observations which indicated the deterioration of the filtrate quality as the extent of deposition becomes significant.

The results on pressure drop increase are shown in Figure 5. The data shown in this figure are in the form of $F_2 - 1$ vs. σ. Results for the HCT and the PCT are essentially the same and are slightly higher than those for the SCT.

Effect of Particle Size. Figures 6 and 7, in which the results obtained using the HCT geometry but with different particles sizes are displayed, show that the effect of particle size on the increase in the collection efficiency, F_1, and in the pressure gradient. $(F_2 - 1)$, was insignificant.

Effect of Initial Filter Bed Porosity. According to the constricted-tube porous media model, the dimensions of the unit cells of a filter bed vary with the porosity of the bed. To determine the possible effect of the initial bed porosity on F_1 and F_2, computations were carried out under the conditions of HCT and N_R = 0.0515 for three porosities (ϵ = 0.38, 0.41, and 0.47) covering the practical range of ϵ in deep bed filters. Results shown in Figures 8 and 9 indicate that this effect appears to be negligible.

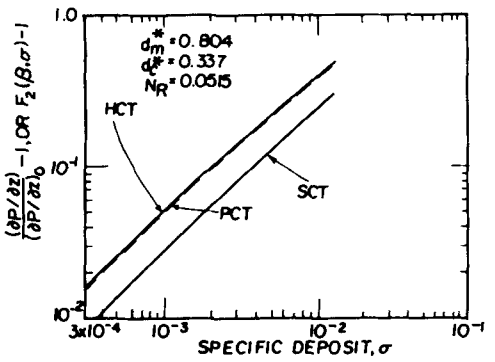

Figure 5. Effect of tube geometry on relationship between $(F_2 - 1)$ and σ-limiting case (A).

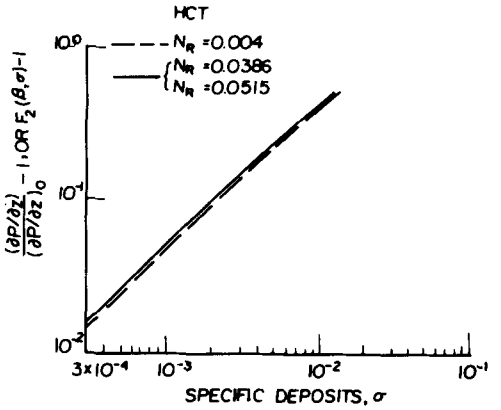

Figure 7. Effect of particle size on relationship of $(F_2 - 1)$ and σ-limiting case (A).

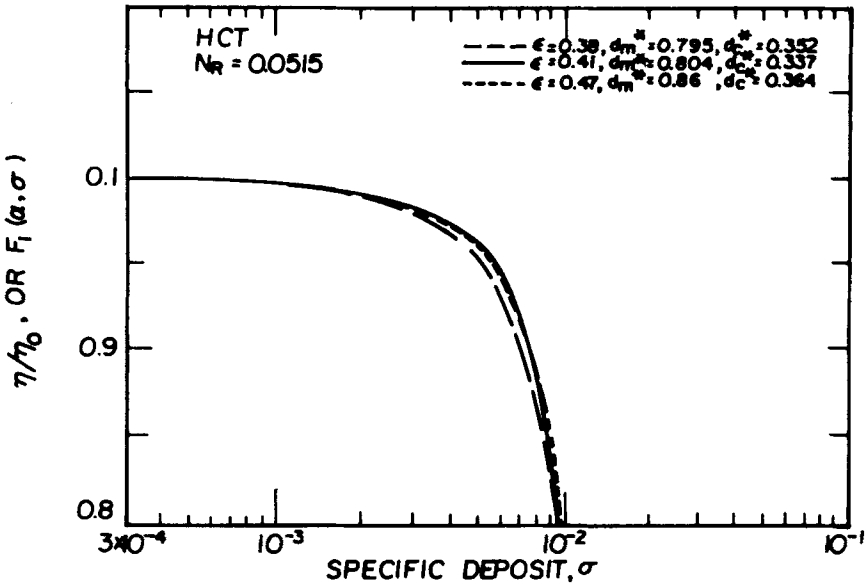

Figure 8. Effect of initial filter bed porosity on relationship between F_1 and σ-limiting case (A).

Limiting Situation (B)

Basic Principles. In contrast to limiting situation (A) presented above, that is, the formation of a smooth coating deposit, one can argue that particle deposits fromed in a filter bed may take on a different configuration, as evident from the model filter experiment of Payatakes et al. (1981). It is therefore necessary to consider the effect of deposited particles not in terms of the overall influence of the particle aggregates upon filter performance but, rather, in terms of the influence of individual deposited particles. This approach has been used in the study of aerosol deposition on fibers (Tien et al., 1977; Wang et al., 1977) and granular aerosol filtration with the use of the constricted-tube porous media model (Pendse and Tien, 1982).

Two basic characteristics—singular and random behavior, and shadow effect—were used to view the particle deposition.

Singular and Random Behavior. From a macroscopic view, the particle concentration of dilute suspensions may be considered uniform. From a microscopic view, however, the locations of the individual particles in the fluid at any instant are stochastic. Furthermore, for the low concentration suspensions commonly encountered in deep-bed filtration, the interference among neighboring particles as they move past a collector surface may be assumed to be negligible. Consequently, to study the deposition of particles from suspensions flowing through a constricted tube (or past a sphere collector), particles may be assumed to enter the tube (or a control plane normal to the direction of the main flow upstream from the sphere collector) one at a time (i.e., to exhibit singular behavior) and at positions randomly distributed over the entire inlet cross section (i.e., to display random behavior).

Shadow Effect. When a particle becomes deposited on the surface of a collector, it may act as an additional collector for subsequent approaching particles. Because of the finiteness of the particle size, the part of the collector surface immediately adjacent to the desposited particle will no longer be accessible to particles for deposition (see Figure 10). This is called the "shadow effect."

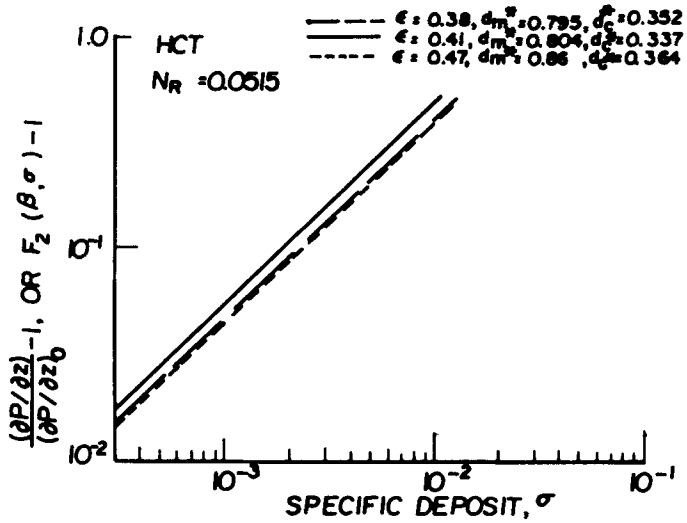

Figure 9. Effect of initial bed porosity on relationship between (F_2 − 1) and σ-limiting case (A).

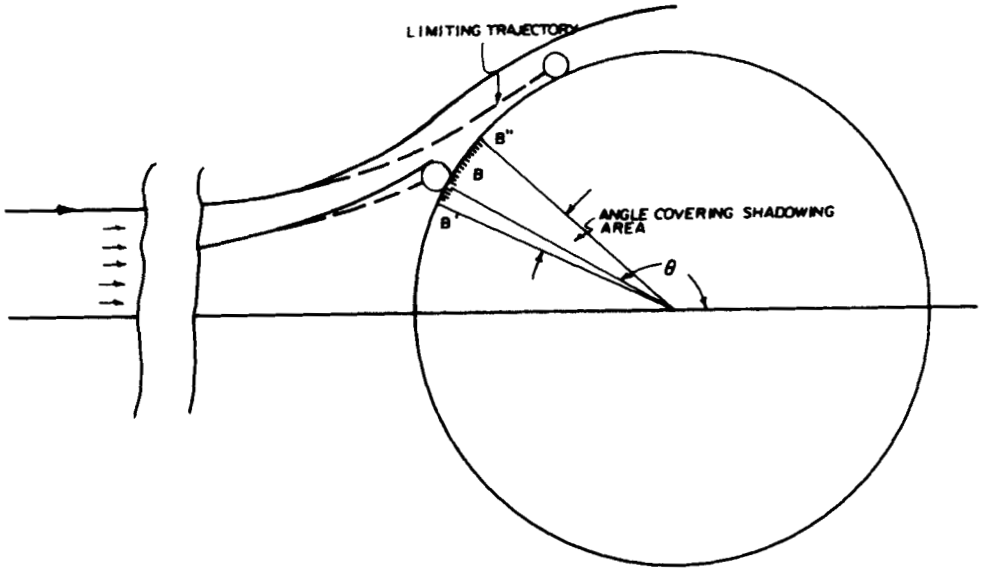

Figure 10. Illustration of shadow effect.

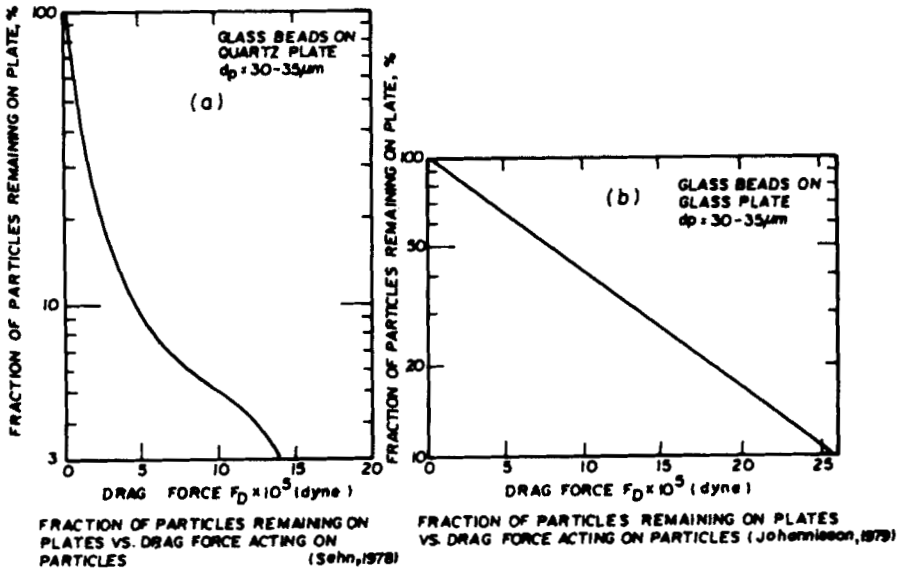

FRACTION OF PARTICLES REMAINING ON PLATES VS. DRAG FORCE ACTING ON PARTICLES (Sehn, 1978)

FRACTION OF PARTICLES REMAINING ON PLATES VS. DRAG FORCE ACTING ON PARTICLES (Johannesson, 1979)

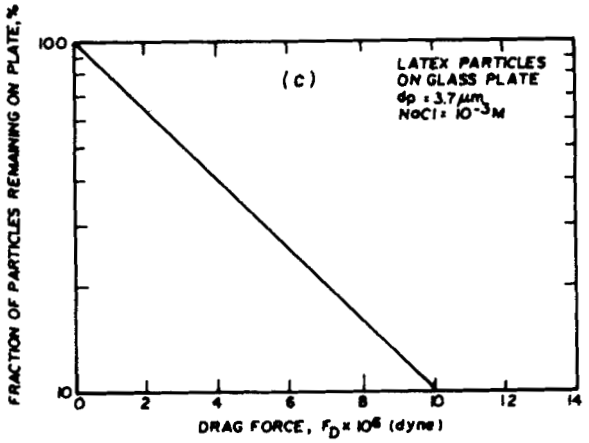

FRACTION OF PARTICLES REMAINING ON PLATES VS. DRAG FORCE ON PARTICLES (Yoshimura, 1980)

Figure 11. Experimental data on adhesion force.

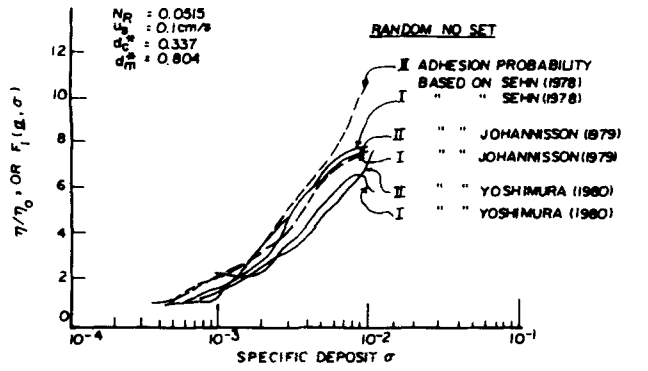

Figure 12. F_1 vs. σ based on different sets of random numbers and adhesion probability measurement data-limiting case (B).

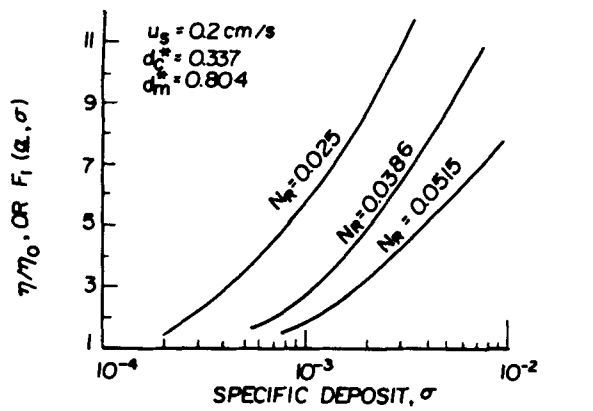

Figure 14. Simulation results of F_1 as functions of σ and N_R-limiting case (B).

The creation of shadow areas by deposited particles has severe implications. First, it means that particle deposition occurs in a discrete manner. Second, it necessitates that particles that ordinarily would have been deposited within the shadow area now be deposited on the deposited particle, leading to the formation of particle aggregates of various sizes and geometries.

These two postulates concerning particle deposition and shadow effect have been confirmed in experiments, for example, in Barot's (1977) work in aerosol deposition on single fibers and in aerosol filtration in model fiber filters by Tsiang et al., (1982).

Simulation Procedure

The procedure for the stochastic simulation used in this work follows closely that described earlier (Pendse and Tien, 1982) with the exception that impacting particles were not automatically collected. Briefly, sequences of pairs of random numbers were generated and were used to determine the inlet positions of the succeeding particles entering a constricted tube of a particular geometry. Once the inlet position of a particle was known, its trajectory as it traveled through the tube could readily be determined on the basis that trajectory coincides with the appropriate streamline. This information in turn determined whether a particle flowed out of the tube, came into contact with the tube wall, or came into contact with a previously deposited particle.

The adhesion probability of a particle impacting upon a collector depends upon the surface conditions of both the particle and the collector and on the nature of the surface interaction forces between them as well as on the flow field around the collector. A predictive capability for the adhesion probability of an impacting particle in terms of the fundamental variables is not available. It is, however, possible to determine experimentally the extent of adhesion by subjecting a collector with deposited particles to a well-defined force field. Such measurement yields results of the percentage of particles adhered vs. the applied force. If the force applied is similar to the force to which impacting particles are subjected in deep-bed filtration, and if one assumes that the particle-collector system used in adhesion measurement is the same as the particle-filter grain system in a deep bed filter, then, for a single impacting particle, the percentage of adhesion vs. force data can be taken to be the adhesion probability of the particle. For a given particle-filter grain system, the likelihood of an impacting particle's becoming collected is determined by the magnitude of the drag force acting on it.

To incorporate the adhesion probability concept into the simulation of deposition of particles in a constricted tube, the following procedure was devised. When a particle entering the constricted tube was found to make contact with the surface of the tube collector or one of the previously deposited particles, the drag force acting on the particle was estimated according to the semiempirical method of Pendse et al. (1981). Based on the value of the drag force, the adhesion probability, γ, was estimated according to the three sets of adhesion data reported by Sehn (1978), Johannisson (1979)

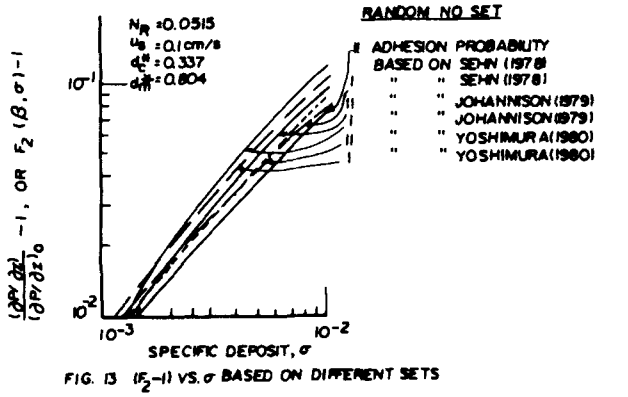

Figure 13. $(F_2 - 1)$ vs. σ based on different sets of random numbers and adhesion probability measurement data-limiting case (B).

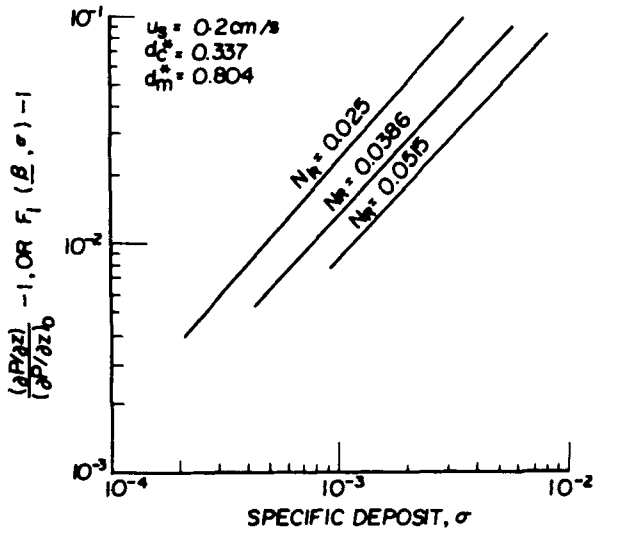

Figure 15. Simulation results of $(F_2 - 1)$ as function of σ and N_R-limiting case (B).

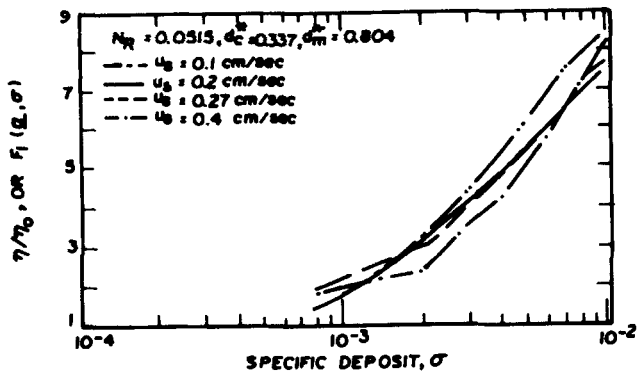

Figure 16. Simulation results of $F_1(\alpha,\sigma)$ as a function of σ and u_s, limiting case (B).

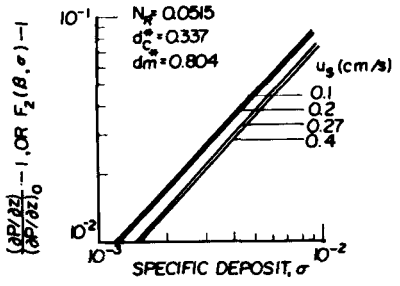

Figure 17. Simulation results of $(F_2 - 1)$ as function of σ and u_s, limiting case (B).

and Yoshimura (1980) (see Figures 11a, b, c). A random number between zero and unity, s, was then generated. If $s \leq \gamma$, then the particle was assumed to be collected. The implicit assumption is that the experimental systems employed by these investigators are representative of the particle filter grain systems encountered in deep-bed filtration. It should be mentioned that these adhesion force measurements (i.e., those works by Sehn, Johannisson, Yoshimura) were made for the particles resting on a flat plate. In view of the fact that filter grains are at least two orders of magnitude larger than the common type of particles to be removed in deep-bed filtration, the use of the plate-sphere model to approximate the grain-particle system in deep bed filters is therefore justified.

The simulation study yields the number of particles collected, M_c, as a function of the number of particles entering the bed, M_{in}, and the positions of the individual deposited particles. By definition, the constricted tube's collection efficiency, η, can be found as

$$\eta = \frac{dM_c}{dM_{in}} \tag{26}$$

and the extent of the deposition described as the specific deposit, σ, is given as

$$\sigma = \frac{(M_c)(\pi d_p^3/3)}{\ell/N_c} \tag{27}$$

Accordingly, the function F_1 can be readily calculated for the definition of F_1 given by Eq. 22a.

To obtain the relationship of F_2 vs. σ, the formula developed earlier (Pendse et al., 1981) can be applied. F_2 is given as

$$F_2 - 1 = \frac{\Delta p}{\Delta p_o} - 1 = \frac{1}{F_{D_o}} \sum_{i=1}^{M_\ell} \Delta F_{D_i}$$

where F_{D_o} is the drag force acting on the surface of the clean constricted tube and can be found readily from the Chow and Soda solution. ΔF_{D_i} is the drag force acting on the ith deposited particles and can be estimated from the procedure of Pendse et al. (1981).

Results

The results presented below were obtained using an SCT geometry with $d_m^* = 0.804$ and $d_c^* = 0.337$. These latter two values were chosen as representative of commonly used filter beds (Payatakes, 1973). Since particle deposition viewed in the present context is a stochastic process, replicate runs of simulation with particle inlet positions corresponding to different sets of random numbers were obtained. The general relationships of F_1 (and $F_2 - 1$) and specific deposit, σ, are shown in Figures 12 and 13. The adhesion probability was estimated from the three different measurements mentioned earlier (Sehn, 1978; Johannisson, 1979; Yoshimura, 1980). These data were used because of their availability and for demonstrating the effect of adhesion only. The use of these different adhesion probability data plus the very nature of stochastic modeling showed that the F_1 (or $F_2 - 1$) obtained varies with the random number set used in simulation as well as with the adhesion force data. Nevertheless, all the results displayed the same qualitative behavior.

Effect of Particle Size. To show the effect of particle size on particle collection and pressure gradient, simulations were made for an SCT, with $u_s = 0.2$ cm/s and each of three particles sizes (i.e., $N_R = 0.025$, 0.0386, and 0.0515). Results are shown in Figures 14 and 15. Figure 14 shows that F_1 increased with σ for all cases. The smaller value of N_R yielded a higher value of F_1. The effect of N_R became more pronounced at higher degrees of deposition.

Figure 15 shows the relationship of pressure gradient (in the form of $F_2 - 1$) and σ for three particle sizes (i.e., $N_R = 0.025$, 0.0386, and 0.0515). Values of $(F_2 - 1)$ increased with σ for all particle sizes. Furthermore, smaller values of N_R yielded higher values of $(F_2 - 1)$.

Effect of Fluid Velocity. Calculations were made using the SCT geometry with $N_R = 0.0515$ and each of four velocities: 0.1, 0.2, 0.27, and 0.4 cm/s. Results shown in Figures 16 and 17 suggest that the fluid velocity does not exhibit a strong influence on either the change in collection efficiency or the pressure drop increase as a filter bed becomes clogged.

Summary

The analyses of the two limiting situations presented above demonstrate convincingly the significance of deposit morphology on filter performance, and the predicted behavior based on them agrees with certain aspects of experimental evidence observed in the past. While neither case completely describes the deposition phenomenon taking place in a real filter, these solutions provide detailed information on the effect of the different operating variables under the limiting conditions. Since physical processes often can be described approximately by a combination of their limiting situations, the availability of these solutions, together with experimental data, affords a way of establishing useful expressions relating the changes in collection efficiency and pressure gradient with the extent of deposition and operating variables, as shown Part II.

ACKNOWLEDGMENT

This study was conducted under National Science Foundation Grant No. CPE-8110760.

NOTATION

c = particle concentration
c_{in} = influent particle concentration
c_∞ = characteristic particle concentration

d_c = constriction diameter of a constricted tube
d_c^* = d_c/d_g
d_g = grain diameter
d_m = maximum diameter of a constricted tube
d_m^* = d_m/d_q
d_p = particle diameter
F_1 = functions defined by Eq. 6
F_2 = functions defined by Eq. 7
F_{Do} = drag force acting on the clean collector
h = height of a constricted tube
I_i = the rate of particle deposition
J_i = particle flux
$g(R),G(R)$ = functions defined by Eqs. 21a and b, respectively
M_c = number of particles collected
M_{in} = number of particles entering the constricted tube
N_c = number of constricted tubes per unit cross-sectional area of filter bed
N_R = d_p/d_g, relative size parameter
$N_{Re,m}$ = $d_g u_m \rho/\mu$, Reynolds number characterizing flow through a constricted tube pressure
p = pressure
P' = P/P_m
P_m = mean wall radius of a constricted tube defined by Eq. 16g
P_m^* = P_m/h
P_o = the farthermost radial position at entrance
P_o^* = P_o/h
P_w = wall radius of a constricted tube
P_w^* = P_w/h
P_w' = P_w/P_m
R = P/P_w
S_{wi} = fraction of irreducible saturation
t = time
t^* = tu_s/d_g, dimensionless time
u_m = $u_s/(\pi P_m^2 N_c)$, mean velocity of flow through a constricted tube
u_s = superficial velocity
$V|_o$ = volume of a clean constricted tube
$V|_{t^*}$ = volume of a constricted tube at t^*
$\hat{V}$ = volume of a single particle present in suspensions
x = coordinate measured tangential to the collector surface
x^* = x/h
y = coordinate measured along the normal direction of the collector surface
y^* = y/h
z = axial coordinate in cylindrical coordinate system
z' = z/P_m
z^* = z/h

Greek Letters

α = parameter vector, see Eq. 6
β = parameter vector, see Eq. 7
Δ = thickness of deposits formed outside filter grains
Δp = pressure drop
$\Delta p'$ = $(\Delta p)P_m/(\rho h u_m^2)$, dimensionless pressure group
δA = surface area element
Δ^* = Δ/d_g
ϵ = bed porosity
ϵ_d = deposit porosity
η = collection efficiency
ℓ = thickness of a unit bed element
λ = filter coefficient
λ_o = initial filter coefficient
μ = fluid viscosity
$\hat{v}$ = volume of a deposited particle
$\hat{v}^*$ = νC_∞, volume concentration of particles
ρ = fluid density
σ = specific deposit, volume of deposited particles per unit bed volume
ψ = stream function
ψ^* = $\psi/(u_s d_g^2)$, dimensionless stream function
ψ' = $\psi/(u_m P_m^2)$, dimensionless stream function
θ = corrected time, see Eq. 5
γ = adhesion probability

LITERATURE CITED

Barot, D., "Formation and Growth of Particle Dendrites on Single Fibers Exposed to Aerosol Flow," M.S. Thesis, Syracuse Univ., Syracuse, NY (1977).

Chiang, H. W., "Transient Behavior of Deep Bed Filtration," Ph.D. Dissertation , Syracuse Univ., Syracuse, NY (1983).

Chow, J. C. F., and K. Soda, "Laminar Flow in Tubes with Constriction," *Phys. Fluuids*, **15**, 1,700 (1972).

Gimbel, R., and H. Sontheimer, "Results on Particle Deposition in Sand Filters," *Deposition and Filtration of Particles from Gases and Liquids*, Society of Chemical Industry, London, 31 (1978).

Herzig, J. P., D. M. Leclerc, and P. LeGoff, "Flow of Suspension through Porous Media—Application to Deep-Bed Filtration," *Ind. Eng. Chem.*, **62**, 8 (1970).

Johannnisson, H., "Untersuchengen zur Veranderung der Partikelhaftung in immergierten systemen durch Polymerzusatz," Thesis, Univ. of Karlsruhe, Karlsruhe, W. Germany (1979).

Lapidus, L., *Digital Computation for Chemical Engineers*, McGraw-Hill, New York (1962).

Lister, M., "The Numerical Solution of Hyperbolic Partial Differential Equations by the Method of Characteristics," *Mathematical Methods for Digital Computers*, A. Ralston and H. S. Wilp, Eds., Wiley, New York, **1**, 165 (1962).

Payatakes, A. C., "A New Model for Granular Porous Media: Application to Filtration through Packed Beds," Ph.D. Dissertation, Syracuse Univ., Syracuse, NY (1973).

Payatakes, A. C., C. Tien, and R. M. Turian, "A New Model for Granular Porous Media. I: Model Formulation," *AIChE J.*, **19**, 58 (1973).

, "Trajectory Calculation of Particle Deposition in Deep Bed Filtration. I: Model Formulation," *AIChE J.*, **20**, 889 (1974).

Payatakes, A. C., H. Y. Park, and J. Petrie, "A Visual Study of Particle Deposition and Reentrainment during Depth Filtration of Hydrosols with Polyelectrolyte," *Chem. Eng. Sci.*, **36**, 1,319 (1981).

Payatakes, A. C., D. H. Brown, and C. Tien, "On the Transient Behavior of Deep-Bed Filtration," AIChE Natl. Meet., Houston, Texas (1977).

Pendse, H., "A Study of Certain Problems Concerning Deep-Bed Filtration," Ph.D. Dissertation, Syracuse Univ., Syracuse, NY (1979).

Pendse, H., and C. Tien, "A Simulation Model of Aerosol Collection in Granular Media," *J. Colloid. Interface Sci.*, **81**, 225 (1982).

Pendse, H., C. Tien, and R. M. Turian, "Drag Force Measurements of Single Spherical Collectors with Deposited Particles, *AIChE J.*, **27**, 364 (1981).

Rajagopalan, R., and C. Tien, "Trajectory Analysis of Deep-Bed Filtration Using the Sphere-in-Cell Porous Media Model," *AIChE J.*, **22**, 523 (1976).

——, "Single Collector Analysis of Collector Mechanisms in Water Filtration," *Can. J. Chem. Eng.*, **55**, 246 (1977).

Sehn, P., "Untersuchengen zur Haftung von Kleiner Glaskugeln auf Quarzplattern in Wassrigen Losungen," Thesis. Univ. of Karlsruhe, Karlsruhe, W. Germany (1978).

Spielman, L. A., and J. A. Fitzpatrick, "Theory for Particle Collection Under London and Gravity Forces," *J Colloid Int. Sci.*, **42**, 607 (1973).

Tien, C., C. S. Wang, and D. T. Barot, "Chainlike Formation of Particle Deposits in Fluid-Particle Separation, *Science*, **196**, 983 (1977).

Tien, C., and A. C. Payatakes, "Advances in Deep-Red Filtration," *AIChE J.*, **25**, 737 (1979).

Tien, C., R. M. Turian, and H. Pendse, "Simulation of the Dynamic Behavior of Deep Bed Filters," *AIChE J.*, **25**, 385 (1979).

Tsiang, R. C., C. S. Wang, and C. Tien, "Dynamics of Particle Deposition in Model Fiber Filters," *Chem. Eng. Sci.*, **37**, 1,661 (1982).

Vanier, C. R., "Simulation of Granular Activated Carbon Columns for Waste Water Treatment," Ph.D. Dissertation, Syracuse Univ., Syracuse, NY (1970).

Wang, C. S., M. Beizaie, and C. Tien, "Deposition of Solid Particles on a Collector: Formulation of New Theory," *AIChE J.*, **23**, 879 (1977).

Yao, K.-M., M. T. Habibian, and C. R. O'Melia, "Water and Waste Water Filtration: Concepts and Applications," *Environ. Sci. Technol.*, **5**, 1105 (1971).

Yoshimura, Y., "A Study of Clarification and Filtration in Packed Beds," Ph.D. Dissertation, Kyoto Univ., Kyoto, Japan (1980).

Manuscript received Feb. 16, 1984; revision received Sept. 17, and accepted Nov. 24, 1984.